

Two-Dimensional Inversion of Papua New Guinea Magnetotelluric Data with Smoothness Regularization

Toshihiro UCHIDA

Geological Survey of Japan, 1-1-3 Higashi, Tsukuba, Ibaraki 305, Japan

(Received March 9, 1995; Revised January 13, 1996; Accepted February 5, 1996)

Two-dimensional inversion has been applied to magnetotelluric data obtained for petroleum exploration in Papua New Guinea. For the inversion, an impedance tensor is rotated to the general strike direction of the area, and TM, TE and determinant impedances are calculated. Distortion-corrected data are also derived to compare the results with the inversion of the original data. The inversion method applied is the linearized least-squares scheme with smoothness regularization. The optimum smoothness is selected based on a statistical criterion, ABIC, which is derived from Bayesian statistics and the maximum entropy theorem. The forward calculation is based on the finite-element method. Topography along the survey line is included in the mesh. The start model is a homogeneous earth, and the final models, obtained by the inversions of TM data, TM and TE data, and determinant data, are generally consistent with each other. A surface high-resistivity layer of 100–1,000 $\Omega\cdot\text{m}$ corresponds to Miocene limestone with a thickness of approximately 1 km. It is underlain by a thick low-resistivity layer of Mesozoic sedimentary rocks which form oil reservoirs.

1. Introduction

Smoothness regularization is commonly applied in various geophysical inversion problems. In this work, the choice of an optimum smoothness is a key factor in obtaining a reliable final model. Constable *et al.* (1987) and deGroot-Hedlin and Constable (1990) introduced an approach to produce the smoothest model for magnetotelluric (MT) inversion which achieves a weighted root-mean-squares (rms) misfit of 1. Smith and Booker (1988, 1991) also proposed a method that seeks a smooth model. Uchida (1993a) utilized a statistical approach to select a suitable smoothness based on ABIC (Akaike's Bayesian Information Criterion), a criterion proposed by Akaike (1980). In this method, once a form of regularization is given, the choice of optimum smoothness is objective and is controlled by the trade-off between the data misfit and model roughness in the process of ABIC-minimization. Uchida (1993b) applied it to two-dimensional (2-D) inversion of a public domain MT dataset, COPROD2, and the feasibility of the method was evaluated. In this paper, the ABIC-minimization scheme is applied to 2-D inversion of magnetotelluric data obtained for oil exploration in a mountainous area in southern Papua New Guinea (PNG).

2. Inversion Method

The inversion algorithm used here is based on the linearized least-squares scheme with a smoothness constraint (Uchida, 1993a). For this method, we have to minimize the functional U ,

$$U = \|Wd - WF(m)\|^2 + \alpha^2 \|Cm\|^2, \quad (1)$$

where W is a weighting matrix, d is observed data, and m is a model. F is a non-linear function which works on the model m to produce MT responses. α is a smoothing parameter, and C is a

roughening matrix. The first term on the right-hand side is the data misfit, and the second term is the model roughness. Since F is non-linear, we first linearize it about a starting model, then modify the model iteratively to minimize U .

The smoothing factor, which is used to trade-off between the contributions of the two terms, needs to be carefully selected. A statistical approach, the ABIC minimization method, is used for this purpose. The ABIC criterion was derived from Bayesian statistics and the maximum entropy theorem (Akaike, 1980; Tarantola, 1987). When applying the Bayesian process to an inversion problem, we define a simultaneous probability density function (pdf) of the misfit minimization and the roughness minimization. A Bayesian pdf (or likelihood), $L(d)$, is defined as

$$L(d) = \int p(d|m)\pi(m) dm, \quad (2)$$

where $p(d|m)$ is a pdf of the misfit minimization and $\pi(m)$ is a pdf of the roughness minimization. When we assume that the observation error is Gaussian with zero mean and variance σ^2 , a pdf of the misfit minimization is given by

$$p(d|m) = \left(\frac{1}{2\pi\sigma^2}\right)^{\frac{N}{2}} \exp\left\{-\frac{1}{2\sigma^2} \|Wd - WF(m)\|^2\right\}. \quad (3)$$

Then, we assume that the spatial derivative of resistivity is Gaussian with zero mean and variance-covariance $\sigma^2 (\alpha^2 C^T C)^{-1}$. A pdf of the roughness minimization is given by

$$\pi(m) = \left(\frac{1}{2\pi\sigma^2}\right)^{\frac{M-1}{2}} |\alpha^2 C^T C|^{\frac{1}{2}} \exp\left(-\frac{\alpha^2}{2\sigma^2} \|Cm\|^2\right), \quad (4)$$

where $|\cdot|$ denotes a determinant of a matrix. Substituting Eqs. (3) and (4) into Eq. (2), we obtain the Bayesian likelihood.

We now seek a model that maximizes the Bayesian likelihood. This is equivalent to the minimization of U . ABIC is defined as follows (Akaike, 1980):

$$\text{ABIC} = (-2) \log(\max L(d)) + 2 \dim(\text{hyperparameters}), \quad (5)$$

where “dim” stands for a dimension of hyper-parameters. The smoothing factor is the only hyper-parameter in this case. The explicit form of ABIC is shown in Uchida (1993a). A smaller ABIC indicates a larger likelihood, hence a better model. The optimum smoothness is obtained in the process of the likelihood maximization. For the derivation of ABIC, we assume that both the misfit and the roughness follow the zero-mean Gaussian process. In an iterative inversion starting from an initial model, the optimum smoothness should be chosen by minimizing ABIC at each iteration.

The forward calculation in two-dimensions is based on the finite-element method. Each of several elements are grouped into an individual block, which is assigned a distinct resistivity treated as an unknown parameter. Topography can be incorporated in the mesh. The sensitivity matrix, consisting of partial derivatives relating changes in model response to perturbation of model parameters, is calculated. This matrix is used, along with the roughening matrix, to predict modifications for each of the parameters. The inversion is iterated until convergence is attained. It is examined by how the rms misfit, parameter modification and ABIC decrease as the iteration proceeds.

The inversion behaves well in reaching stable convergence for many cases, when the assumptions of Gaussian noise and two-dimensionality are valid practically. However, on occasion, ABIC and/or the rms misfit become greater than that of the previous iteration after several iterations.

This may be caused by a breakdown of the local linearity assumption for partial derivatives. In such a case, a damping operation is essential to adjust the model step, by adding a constant to the diagonal elements of the roughening matrix. The optimum damping is also chosen based on the ABIC minimization.

3. Data and Inversion

The PNG data were obtained from the Kube-Kabe magnetotelluric project for petroleum exploration carried out in 1991 in a southern highland of Papua New Guinea. The survey area is underlain by a thick layer of Darai limestones of Miocene age (Christopherson, 1991). It overlies thicker sedimentary rocks of Jurassic and Cretaceous ages. These formations were folded by a northeast-southwest directed compression, and many thrust fault systems were created. Oil reservoirs were then formed in the Mesozoic formations. Therefore, both the geology and topography have strikes of a northwest-southeast trend. Three survey lines were arranged to cross the geologic strike in the Kube-Kabe survey, and the data of the Wara survey line is used in this work. The data consist of ten stations along a northeast-southwest survey line (Fig. 1). A 2-D assumption seems to be valid according to the geologic setting and topography.

Ogawa (1997) applied distortion decomposition (Groom and Bailey, 1989) to the original MT impedance by assuming that the strike direction is the same for all frequencies and all sites. The general strike direction obtained by decomposition was -66 degrees. The survey line is not

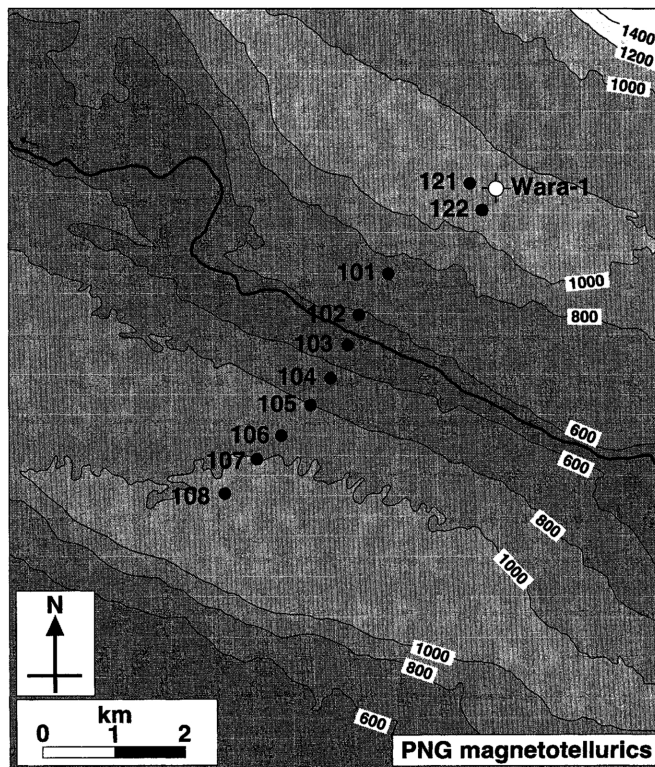


Fig. 1. The PNG magnetotelluric sites (solid circles) on a topography map. Elevations are shown in meters.

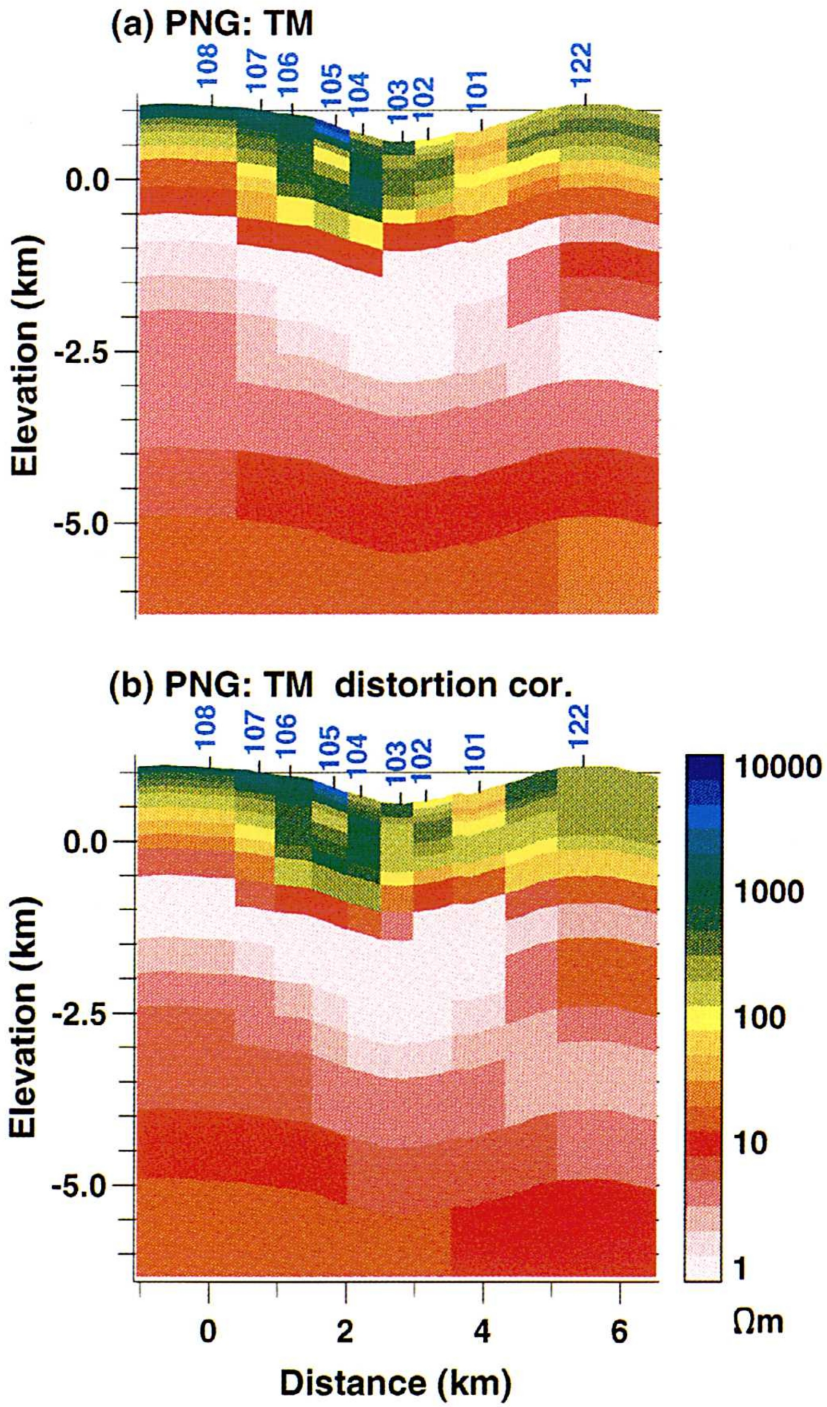


Fig. 2. Inverted models of the PNG data for (a) original TM data, (b) distortion-decomposed TM data, (c) original determinant data and (d) original TM/TE data. A 3% noise floor is assumed.

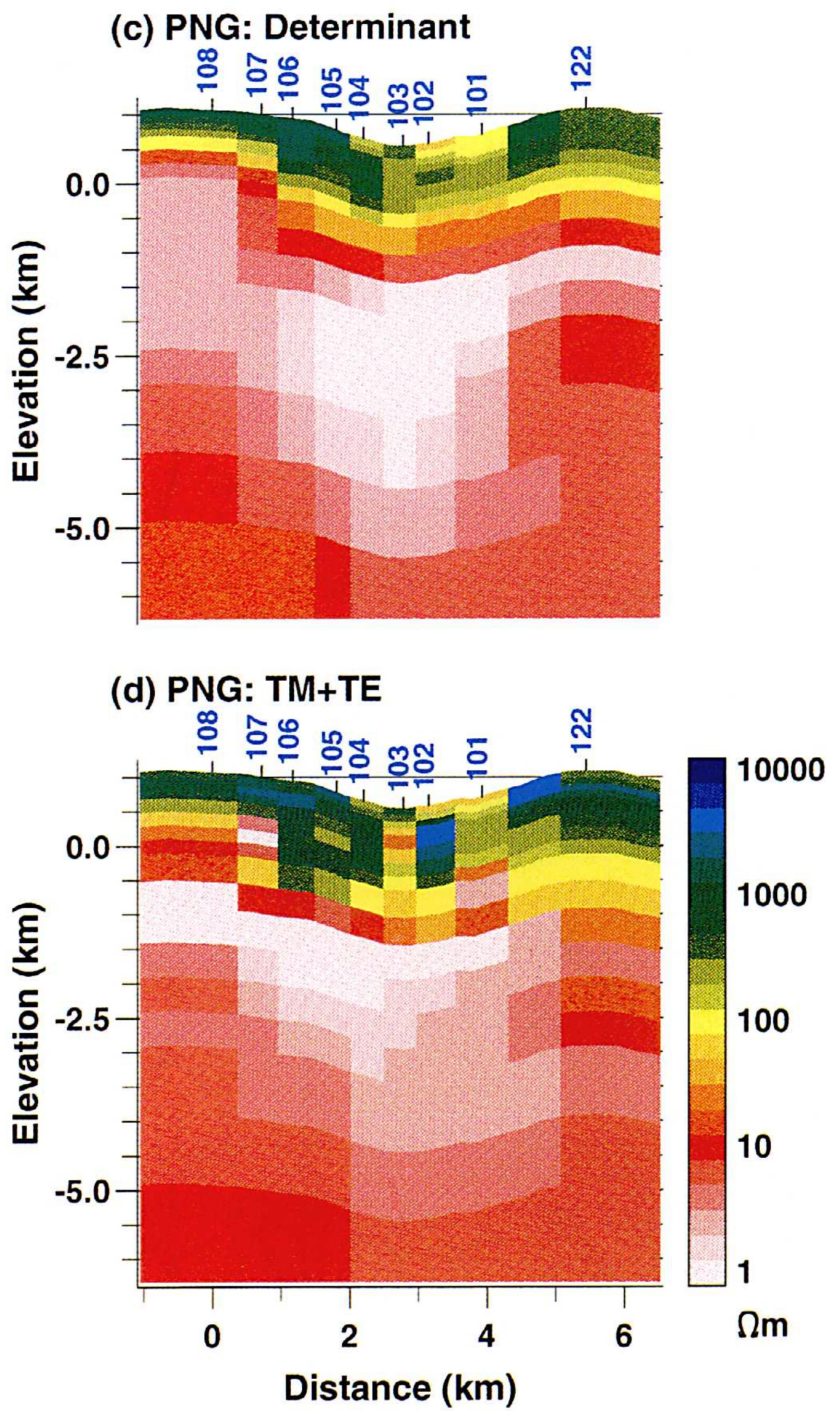


Fig. 2. (continued).

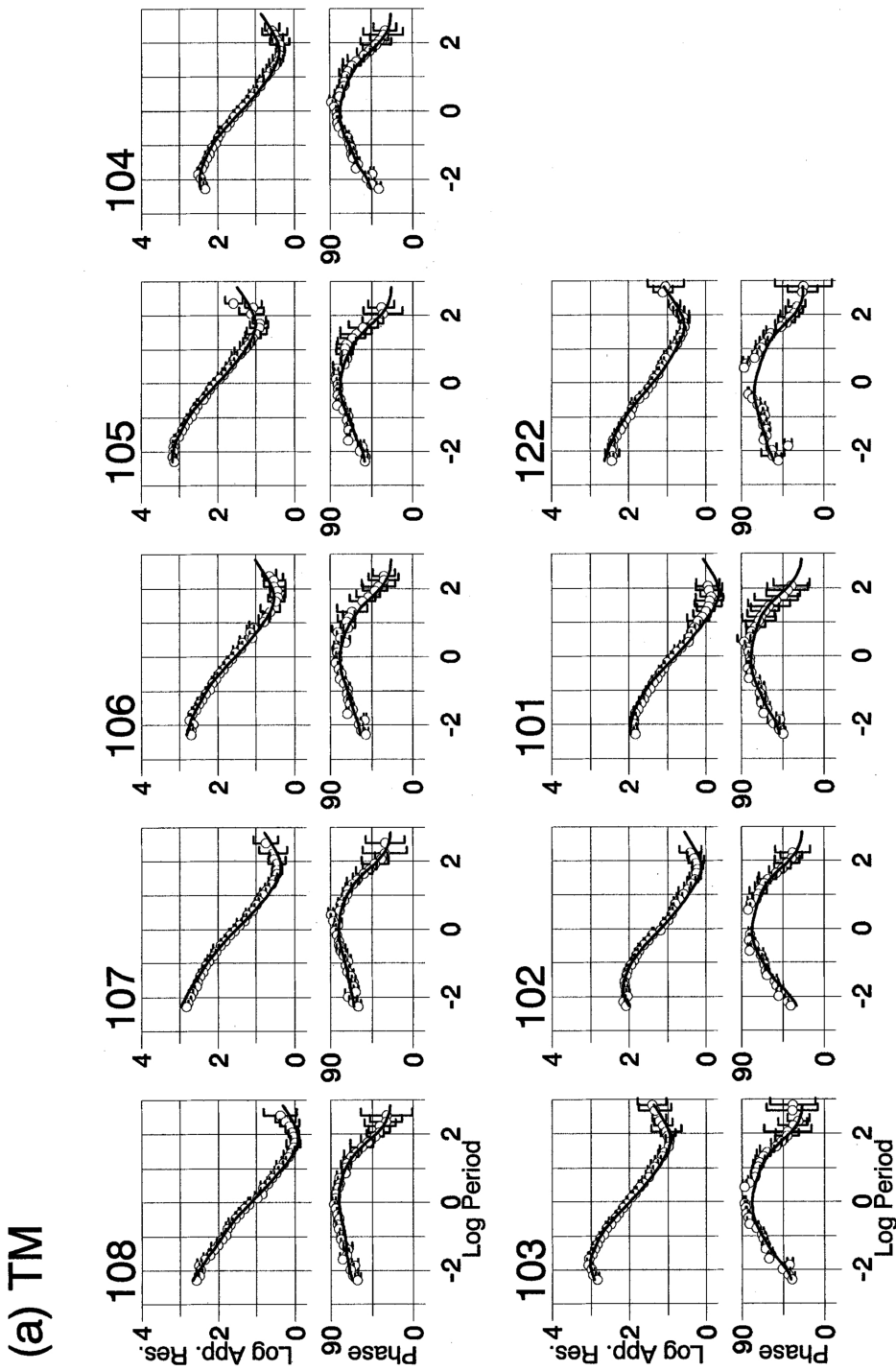


Fig. 3. Observed apparent resistivities and phases (open circles) and calculated ones from the model by the TM/TE inversion shown in Fig. 2(d) (solid lines); (a) TM data and (b) TE data. Fitting for the TE apparent resistivity is ignored in the inversion. Observation errors of one standard deviation are also shown by vertical bars.

(b) TE

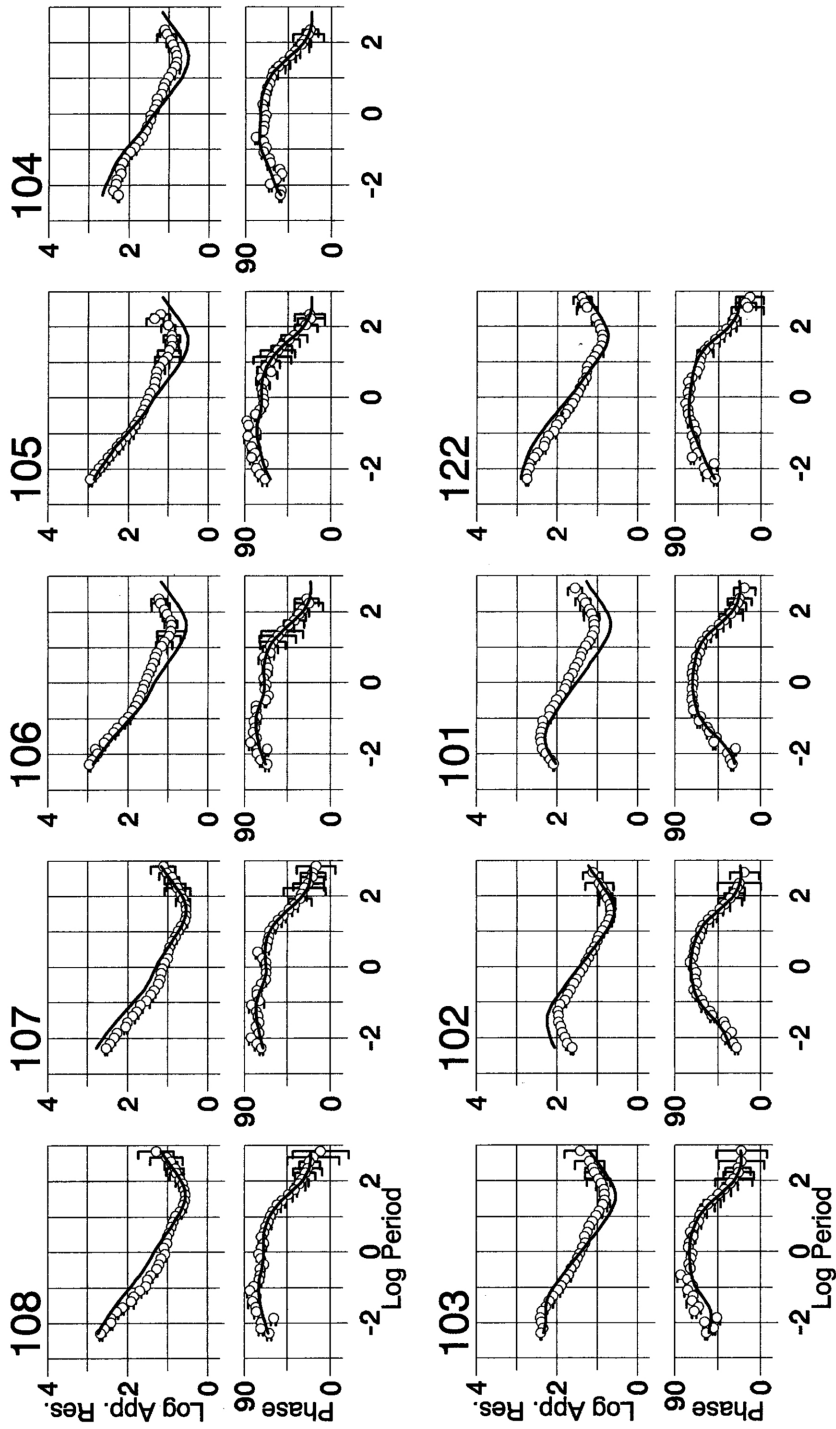


Fig. 3. (continued).

precisely perpendicular to the strike, however, I use impedances which are decomposed for twist and shear and are rotated to the strike direction as one set of data. Also, to compare the effect of distortion on the inverted model, the original data are rotated to the direction of -66 degrees, and TM, TE and determinant impedances are then calculated. Local 3-D galvanic distortion is not severe for this dataset. The correction is generally less than 2% for apparent resistivity and less than 1 degree for phase, except for several large corrections for low frequency data and for Sites 103 and 122.

The number of frequencies used for the inversion is 35, ranging from 0.00147 Hz to 192 Hz. Noisy data, whose observation error is greater than 200% in apparent resistivity and 32 degrees in phase, are omitted. The original TM, TE and determinant data, and the distortion-corrected TM data, are used for the inversion. Since Sites 121 and 122 are closely located, and both of them cannot fit a 2-D model simultaneously, only Site 122 is used in this work. The number of data used, counting apparent resistivity and phase separately, is approximately 560 for each mode.

The forward modeling is accomplished using the finite-element method. Since the line crosses a relatively steep hill and valley, topography should be taken into account in the modeling. Elevations along the survey line were read from a survey map, and are incorporated into the finite-element mesh. Each node of the mesh is shifted according to the elevations of the surface nodes. The sizes of the surface elements are 50 m vertically and no larger than 100 m horizontally.

The subsurface medium is divided into 205 blocks, each of which is assigned a distinct resistivity. The blocks are arranged so that each station is assigned one column of blocks. However, one additional column is added between Sites 101 and 122 as the inter-station spacing between them is too large. The initial model is a $100 \Omega\cdot\text{m}$ homogeneous earth. A smoothness constraint with a 2-D Laplacian roughening operator is applied. The roughening operator is weighted according to the horizontal and vertical sizes of a block; the form of the roughening matrix is given in Uchida (1993a). A noise floor of 3% is assumed for the weighted least-squares inversion. For the determinant inversion, the determinant of the impedance tensor is used as observed data, and the geometric mean of numerical TM and TE values is used as a theoretical response.

4. Two-Dimensional Models

Figure 2 compares four inverted models for (a) original TM data, (b) distortion decomposed TM data, (c) original determinant data and (d) original TM/TE data (TM data combined with TE data). The inversion using TE apparent resistivity does not produce a realistic earth model, mainly because static shift and three-dimensionality of the TE data are difficult to deal with properly in two dimensions. Therefore, only phases are used for the TE data of the TM/TE inversion (Fig. 2(d)). The observed and theoretical apparent resistivities and phases for the inversion of the TM/TE data are shown in Fig. 3.

The models, for the distortion-corrected and non-corrected TM mode data, are almost identical (Figs. 2(a) and 2(b)). This is because the local 3-D galvanic distortion is not large. Some minor differences are recognizable at the deeper portion on the right-hand side of the sections. The determinant inversion (Fig. 2(c)) gives a slightly different model from the TM models. The surface resistive layer is a little thinner, and the low-resistivity anomaly is concentrated in the middle of the section. The shallow blocks in the TM/TE inversion model are not very realistic, as the resistivities vary site by site. For example, a low-resistivity block exists beneath Site 107. On the other hand, the deeper blocks are similar to the TM models.

The topography effect is not negligible for the steep terrain along the line. For example, a test to check the topography effect with a $100 \Omega\cdot\text{m}$ homogeneous earth gives an apparent resistivity of approximately $200 \Omega\cdot\text{m}$ for low frequency data at Site 103. However, an inversion with a flat topography (not shown) produces a similar model to that of a topography-incorporated inversion. The topography effect seems to be compensated for with the resistivity variation of the shallow

layer. Thus, the resistivities of deeper blocks are unaffected.

The four models are basically very similar to each other. Besides the fact that the TE apparent resistivity can not be explained properly with a realistic 2-D model, we can rely on the common features of these models as depicting true underground structures.

According to a geology section along the survey line (Jones, 1994), the Darai limestones outcrop throughout the survey line and thicken slightly northeastward (to the right on the model) as a result of thrust faulting. Since the limestones are resistive (Christopherson, 1991), we can interpret that the shallow resistive layer of 100–1,000 $\Omega\cdot\text{m}$ corresponds to the Darai. The thickness of the layer varies site by site. However, it is approximately 1 km throughout the line.

The limestone layer is underlain by a very conductive and thick layer of 1–3 $\Omega\cdot\text{m}$. This is interpreted as Mesozoic sedimentary rocks which form hydrocarbon-bearing zones. In the models, we can recognize a small resistive block in the conductive layer beneath Site 122. This may be due to Darai limestone left deep by a thrust fault. Underlying the conductive layer is a resistive basement which inclines rightward on the sections. Its depth is not clear in the models, but it is 3–5 km below sea level.

5. Conclusions

Two-dimensional inversions, with smoothness constraint, were performed for the PNG magnetotelluric data, both for the original and decomposed data. Since local 3-D galvanic distortion is not so large in the data, the models are not significantly different.

The models by the inversions of TM data, determinant data and TM/TE data are basically similar to each other. Features common among the resistivity models are as follows. A surface high-resistivity layer of 100–1000 $\Omega\cdot\text{m}$ is interpreted as the Darai limestones of Miocene age. Its thickness is approximately 1 km. It is underlain by a thick low-resistivity layer of sedimentary rocks of Jurassic and Cretaceous ages, which form oil reservoirs. The resistivity of this zone is as low as 1–3 $\Omega\cdot\text{m}$. A high-resistivity basement is seated at a depth of approximately 3–5 kilometers below sea level.

The author is grateful to C. M. Swift of Chevron Overseas Petroleum Inc. and A. G. Jones of the Geological Survey of Canada for providing the PNG data, and to Y. Ogawa of the Geological Survey of Japan for providing the decomposed data.

REFERENCES

- Akaike, T., Likelihood and Bayes procedure, in *Bayesian Statistics*, edited by Bernardo, J. M., M. H. deGroot, D. V. Lindley, and A. F. Smith, pp. 143–166, University Press, Valencia, Spain, 1980.
- Christopherson, K. R., Applications of magnetotellurics to petroleum exploration in Papua New Guinea: A model for frontier areas, *Leading Edge*, **10-4**, 21–27, 1991.
- Constable, S. C., R. L. Parker, and G. Constable, Occam's inversion: a practical algorithm for generating smooth models from electromagnetic sounding data, *Geophysics*, **52**, 289–300, 1987.
- deGroot-Hedlin, C. and S. C. Constable, Occam's inversion to generate smooth, two-dimensional models from magnetotelluric data, *Geophysics*, **55**, 1613–1624, 1990.
- Groom, R. W. and R. C. Bailey, Decomposition of magnetotelluric impedance tensors in the presence of local three-dimensional galvanic distortion, *J. Geophys. Res.*, **94-B2**, 1913–1925, 1989.
- Jones, A. G., Overview of PNG magnetotelluric data, Paper presented at *Second Magnetotelluric Data Interpretation Workshop (MT-DIW2)*, held in Cambridge, England, August 5–6, 1994.
- Ogawa, Y., Two-dimensional inversion of Papua New Guinea magnetotelluric dataset assuming static shift as a Gaussian distribution, *J. Geomag. Geoelectr.*, **49**, this issue, 857–867, 1997.
- Smith, J. T. and J. R. Booker, Magnetotelluric inversion for minimum structure, *Geophysics*, **53**, 1565–1576, 1988.
- Smith, J. T. and J. R. Booker, Rapid inversion of two- and three-dimensional magnetotelluric data, *J. Geophys. Res.*, **96-B3**, 3905–3922, 1991.
- Tarantola, A., *Inversion Problem Theory*, Elsevier, Amsterdam, 1987.

- Uchida, T., Smooth 2-D inversion for magnetotelluric data based on statistical criterion ABIC, *J. Geomag. Geoelectr.*, **45**, 841–858, 1993a.
- Uchida, T., Inversion of COPROD2 magnetotelluric data by use of ABIC minimization method, *J. Geomag. Geoelectr.*, **45**, 1063–1071, 1993b.